High-dimensional flow-cytometric analysis of human B-cell populations

The BD FACSCelesta™ cell analyzer and FlowJo™ software together enable deep analysis of B-cell biology

Features

- High-resolution analysis of over 7 distinct B-cell subsets using a 12-color panel

- Evaluation of distinct B-cell populations across different tissue types

- Robust data analysis using the t-SNE analysis feature of FlowJo™ v10 software

B-cell development is a stepwise process initiated in the fetal liver and postnatal bone marrow and continued in the peripheral lymphoid organs upon encounter with antigens. The various stages of B-cell differentiation can be identified by evaluating the expression and levels of distinct cell-surface markers, which are regulated throughout the course of B-cell differentiation.

Multicolor flow cytometry is a powerful tool that has driven key discoveries in B-cell biology by facilitating the investigation of B-cell markers during cell development, differentiation and pathologies such as immunodeficiency, autoimmune disorders and malignancies.

This datasheet describes a 12-color flow cytometry panel for the analysis of the most prominent B-cell subsets in human peripheral blood and bone marrow. The 12-color panel included markers uniquely expressed in certain cell subsets such as CD138 in plasma cells, as well as co-expressed markers (CD38 and CD24) (Figure 1A). The panel was designed to identify immature/transitional subsets (T1, T2 and T3), naive B cells, memory B-cell subsets, plasmablasts and plasma cells. The cells in the naive B-cell subset that uniquely express the ATP-binding cassette B1 (ABCB1) transporter were identified by analysis of cell extrusion of MitoTracker™ Green FM (ThermoFisher), a green-fluorescent mitochondrial stain. Anti-CD3 and 7-AAD were included to allow accurate gating of viable, CD19⁺ lineage-specific B cells. The BD FACSCelesta™ multicolor analyzer enabled the use of up to six BD Horizon Brilliant™ Violet dyes, two BD Horizon Brilliant™ Ultraviolet dyes and four additional dyes for the best resolution of the critical B-cell populations (Figures 1B and 1C).
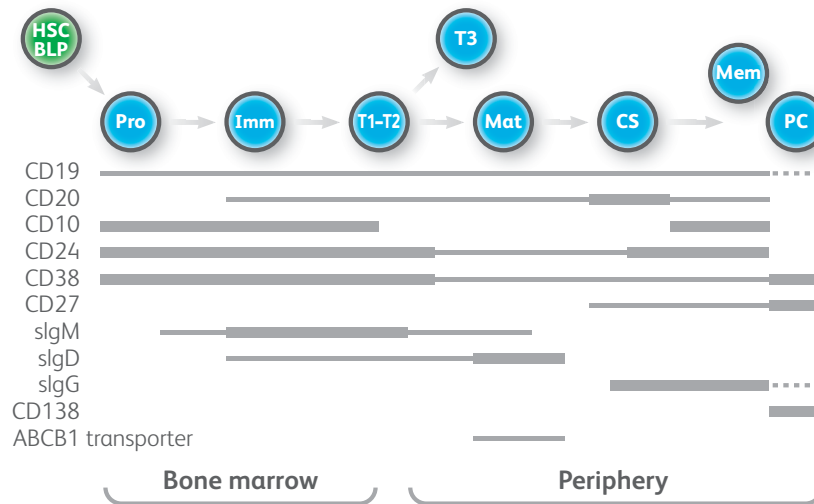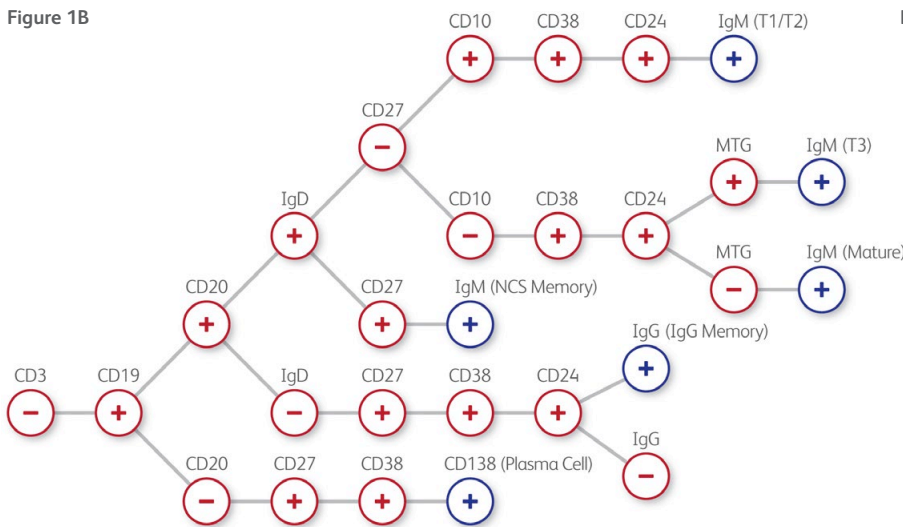
Figure 1A

Figure 1B

Figure 1C

Laser (nm)	Fluorochrome	B-Cell Panel
355	BUV737	CD138
Ultraviolet	BUV395	IgM
	BV786	CD20
	BV711	CD10
405	BV650	IgG
Violet	BV605	CD27
	BV480	IgD
	BV421	CD38
	PE-Cy™7	CD19
488	PerCP-Cy™5.5	CD3 & 7-AAD
Blue	PE	CD24
	*MTG	MTG

*MitoTracker™ Green FM

Figure 1. Design of a 12-color panel for the analysis of human B-cell subsets

A. Schematic representation of various B-cell subsets, showing the expression profile of cell-surface markers detected using a 12-color panel. The relative expression levels of the phenotypic markers throughout cell development and differentiation are indicated: thickness of the line indicates the level of expression and dashed lines indicate diminished expression. The B-cell maturation and differentiation pathway includes hematopoietic stem cells and B-lineage progenitors (HSC/BLP), B-cell progenitors and precursors (Pro), immature (Imm), transitional (T1, T2 and T3), mature (Mat), class-switched (CS) and memory (Mem) B cells and plasma cells (PC). **B**. Representative diagram, showing a B-cell population hierarchy that was generated using the BD Horizon™ Guided Panel Solution (GPS). The critical B-cell populations including non-class-switched (NCS) memory are indicated in blue. **C**. B-cell panel for analysis in the BD FACSCelesta™ multicolor analyzer equipped with blue, violet and ultraviolet lasers.

The experimental data was analyzed using FlowJo v10 software, which comes with a series of plug-ins (applications) for analysis and visualization of high-dimensional data, in addition to measuring the B-cell populations in bivariate contour plots.

Figure 2 illustrates our gating strategy for comparing B-cell populations in peripheral blood mononuclear cells (PBMCs) and bone marrow mononuclear cells (BMMCs). Initially, live B cells were identified as 7-AAD$^-$CD3$^-$CD19$^+$ cells. Then, analysis of CD38 versus CD10 expression within the CD19$^+$ population revealed three main B-cell subsets: CD38^{high}CD10$^-$, CD38^{high}CD10^{high} and CD38^{low}CD10$^-$. The proportions of CD38^{high}CD10^{high} cells, which correspond to immature B cells and B-cell progenitors, were high in the BMMCs as compared to PBMCs. Only a small proportion of CD38^{high}CD10^{high} cells was observed in PBMCs and likely corresponds to transitional cells that recently emerged from the bone marrow.
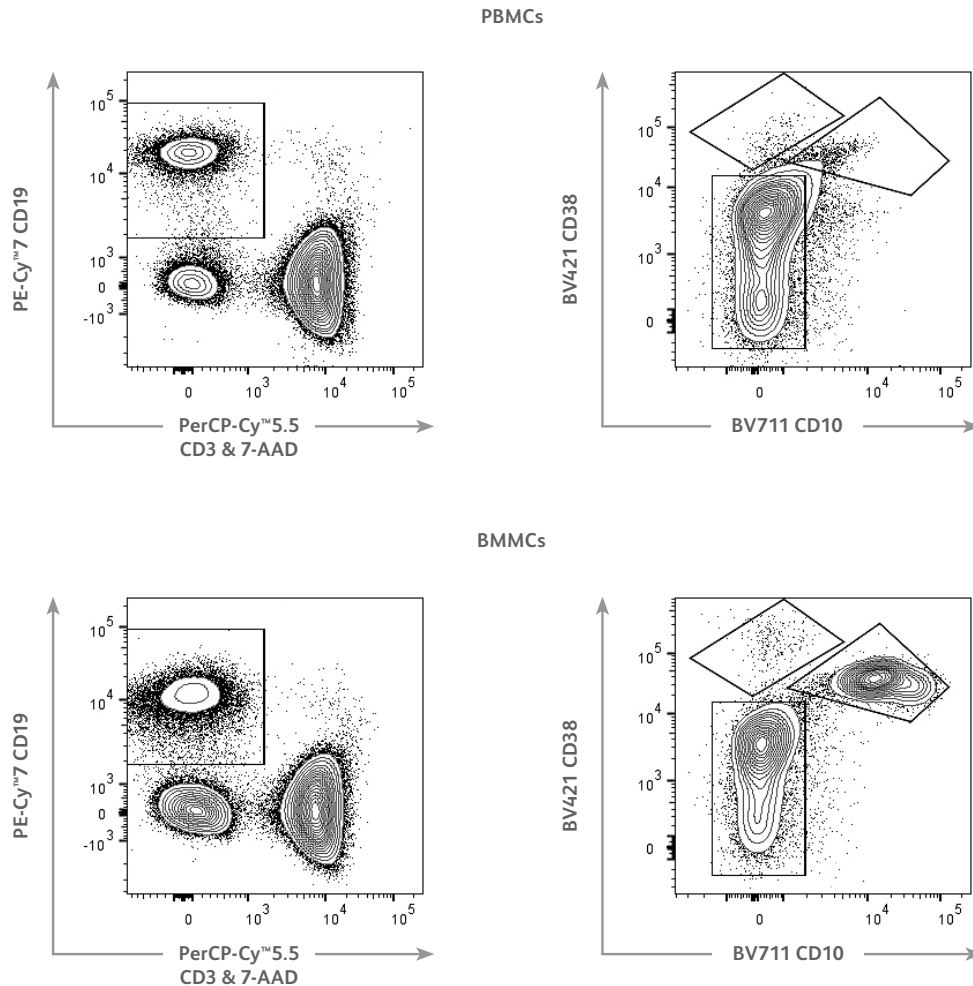
Figure 2

PBMCs

BMMCs

Figure 2. Analysis of B-cell subsets in human peripheral blood and bone marrow with a 12-color panel

PBMCs or frozen BMMCs were prelabeled with MitoTracker Green for 30 min and chased for 30 min with culture medium. After washing, the cells were stained with a cocktail containing BD Horizon™ Brilliant Stain Buffer Plus and the following anti-human antibodies: CD3, CD19, CD10, CD20, CD24, CD27, CD38, CD138, IgM, IgD and IgG. Prior to acquisition by the BD FACSCelesta system, the cells were washed and re-suspended in solution containing BD Pharmingen™ 7-AAD to enable determination of cell viability. The figure shows a comparative analysis between mononuclear cells from peripheral blood and bone marrow. Based on the expression of CD38 and CD10 in gated live CD19$^+$ B cells, three major B cell subsets were identified: CD38^{high}CD10$^-$, CD38^{high}CD10^{high}, and CD38^{low}CD10$^-$. The remaining phenotypic markers in the panel were used for a comprehensive analysis of all B-cell subsets in both tissues, as shown in figures 3 and 4.

To achieve a comprehensive analysis of the different B-cell subsets identified by our panel, we performed t-Distributed Stochastic Neighbor Embedding (t-SNE) in the FlowJo software. This allowed automatic identification of the B-cell populations for simpler comparison between bone marrow cells and PBMCs across different donors. During cell analysis, the numbers of gated CD19$^+$ B cells from two donors were reduced to an equal number of cell events, a process known as downsampling. Then, the downsampled events were concatenated in one single file and analyzed using t-SNE. Downsampling is necessary to reduce the processing time of this version of the data reduction algorithm in t-SNE.

The five major groups of B cells—mature, class-switched memory, non-class-switched memory, transitional and plasmablasts—were identified in PBMCs using t-SNE. Also, a smaller subset of IgG⁺ class-switched memory cells was detected, as well as a rare population of CD138⁺ plasma cells. The transitional cell subsets, T1–T2 and T3 could be distinguished according to the differential expression of MTG, CD24, CD38 and CD10 (Figure 3A). Similarly, BMMCs also contained distinct clusters of mature B cells, CD27⁺ memory B-cell subsets and plasmablasts. In contrast to PBMCs, in the bone marrow we detected larger clusters of CD10-expressing B cells that could be subdivided into CD10^{bright} and CD10^{dim} B cells (Figure 3B).
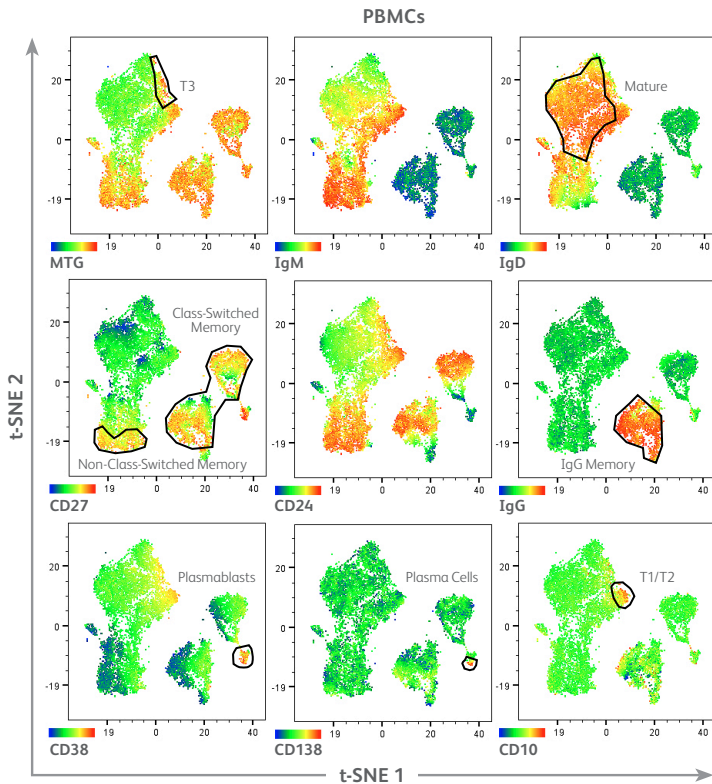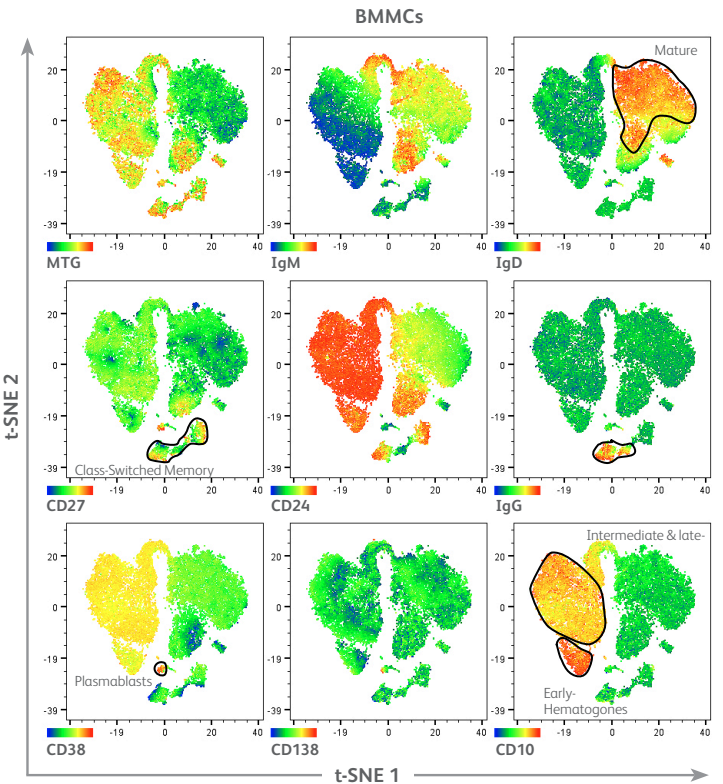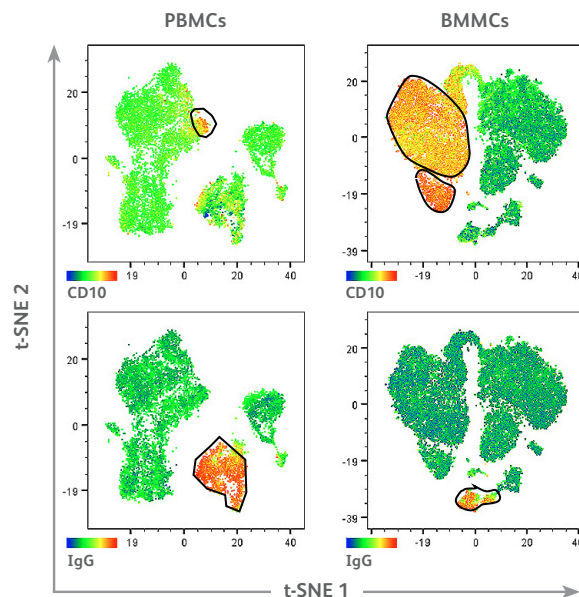

Figure 3. High-dimensional flow cytometry analysis of human B-cell subsets

PBMCs or frozen BMMCs stained in Figure 2 were visualized in two-dimensional t-SNE plots for the indicated phenotypic markers. The intensity of the shades of blue and red indicates a gradient of expression from low to high levels. **A.** PBMC samples from 2 donors were run independently and a total of 10,000 CD19⁺ events from each donor were concatenated in one single file prior to applying t-SNE analysis in FlowJo. **B.** Frozen BMMCs were stained with the same antibody cocktail and analyzed in parallel to PBMCs. As indicated in Figure 3A, mature, class-switched memory, non-class-switched memory and transitional B cells and plasmablasts were identified among PBMCs. Also, IgG⁺ B cells and CD138⁺ plasma cells were clearly distinguished and the transitional B cell subsets could be further divided into T1-T2 and T3 cells. **B and C.** BMMCs contained the same B-cell subsets found in the peripheral blood and additionally presented a large compartment of CD19⁺IgM⁻CD24⁺CD38⁺CD10⁺ cells.

The use of t-SNE analyses also allowed us to easily detect downregulation of CD10 expression during B-cell maturation. CD10 thus is a key marker in our panel to evaluate the progression of B-cell maturation from early stages in the bone marrow to mature stages in the periphery, whereas other markers (such as IgG) demonstrate the circulation of B-cell subsets through the different tissues (Figure 3C).

As B cells mature from $CD10^{bright}$ to $CD10^-$ mature B cells, they also upregulate the expression of CD20. Analysis of CD10 versus CD20 expression in bivariate plots revealed the various stages of B-cell maturation from precursors or hematogones to more mature B cells: early- ($CD10^{bright} CD20^-$), intermediate- ($CD10^+ CD20^{-/low}$) and late-hematogones ($CD10^+ CD20^+$) and mature B cells ($CD10^- CD20^+$). Nonetheless, t-SNE clustering analysis provided a much more robust separation of the cell populations than the bivariate analysis, further demonstrating the significance of t-SNE for visualization of rare cell populations (Figure 4).
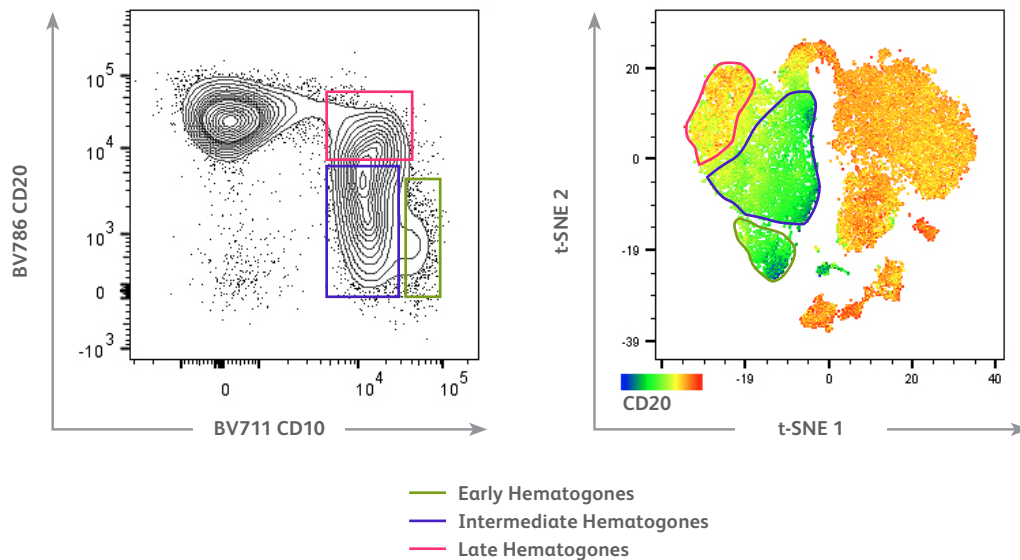
Figure 4

— Early Hematogones
— Intermediate Hematogones
— Late Hematogones

Figure 4. Deep analysis of B-cell progenitors in the bone marrow
Frozen BMMCs stained in Figure 2 were further analyzed in bivariate (left) and t-SNE (right) plots. Examination of the correlated expression of CD10 and CD20 in $CD19^+$ cells demonstrated the normal B-cell maturation pattern from early-stage hematogones ($CD10^{bright} CD20^-$), through an intermediate stage ($CD10^+ CD20^{-/low}$) to a late stage ($CD10^+ CD20^+$). The hematogones were also clearly distributed into three distinct populations in the t-SNE plot showing CD20 expression, though they are more difficult to separate in the bivariate plot.

In summary, using a 12-color panel, we created a list of lineage and differentiation markers for a detailed analysis of B-cell differentiation stages in peripheral blood and bone marrow. The backbone of the panel, comprising CD19, CD27, IgM, IgD, CD24, CD38, CD20, CD3 and 7-AAD, was used to detect the major B-cell populations while the additional markers, MTG, CD10, IgG and CD138 were used to further distinguish unique B-cell subsets. Use of the t-SNE algorithm from the FlowJo platform provided simultaneous analysis of independently run samples from different donors and simplified comparison of cell distribution between different tissues. Importantly, t-SNE automatically created cell clusters in an unbiased manner and enabled visualization of rare populations, such as plasma cells. Hence, the combination of a high-performance instrument and the proper tools and practices for analysis of high-dimensional data provides a robust and efficient single solution approach for cell analysis.

Ordering information

Systems and software	
Description	**Cat. No.**
BD FACSCelesta™ Flow Cytometer System, Blue, Violet and Ultraviolet (BVUV) Configuration	660346
FlowJo™ v10.4.1 or greater	—

Reagents		
Description	**Clone**	**Cat. No.**
BD Horizon™ Brilliant Stain Buffer Plus	—	566385
BD Pharmingen™ PerCP-Cy™5.5 Mouse Anti-Human CD3	UCHT1	560835
BD OptiBuild™ BV711 Mouse Anti-Human CD10	HI10a	740770
BD Pharmingen™ PE-Cy™7 Mouse Anti-Human CD19	HIB19	560728
BD OptiBuild™ BV786 Mouse Anti-Human CD20	L27	740838
BD Pharmingen™ PE Mouse Anti-Human CD24	ML5	555428
BD Horizon™ BV605 Mouse Anti-Human CD27	L128	562655
BD Horizon™ BV421 Mouse Anti-Human CD38	HIT2	562444
BD Horizon™ BUV737 Mouse Anti-Human CD138	MI15	564393
BD Horizon™ BV480 Mouse Anti-Human IgD	IA6-2	566138
BD OptiBuild™ BV650 Mouse Anti-Human IgG	G18-145	740596
BD Horizon™ BUV395 Mouse Anti-Human IgM	G20-127	563903

BD Life Sciences, San Jose, CA, 95131, USA

bdbiosciences.com